Percolation of sticks: Effect of stick alignment and length dispersity

Yuri Yu. Tarasevich* and Andrei V. Eserkepov†
Laboratory of Mathematical Modeling, Astrakhan State University, Astrakhan 414056, Russia

(Received 16 November 2018; published 27 December 2018)

Using Monte Carlo simulation, we study the percolation of sticks, i.e., zero-width rods, on a plane, paying special attention to the effects of stick alignment and their length dispersity. The stick lengths are distributed in accordance with log-normal distributions, providing a constant mean length with different widths of distribution. Scaling analysis is performed to obtain the percolation thresholds in the thermodynamic limits for all values of the parameters. Greater alignment of the sticks leads to increases in the percolation threshold, while an increase in length dispersity decreases the percolation threshold. A fitting formula is proposed for the dependence of the percolation threshold both on stick alignment and on length dispersity.

DOI: 10.1103/PhysRevE.98.062142

I. INTRODUCTION

Percolation, i.e., the occurrence of a connected subset (a cluster) within a disordered medium which spans its opposite borders, has attracted the attention of the scientific community over several decades [1–5]. Nowadays, two-dimensional (2D) systems such as transparent electrodes present examples of where highly conductive particles, e.g., nanowires (NWs), nanotubes (NTs), and nanorods (NRs), form a random resistor network inside a poorly conductive host matrix (substrate) [6–8]. The appearance of a percolation cluster in these kinds of systems drastically changes their physical properties and is associated with an insulator-to-conductor phase transition. Length dispersity is common for NWs, NTs, and NRs [9–12]. These works evidenced that the length distributions of NWs, NTs, and NRs are close to representing log-normal distributions. Furthermore, the alignment of such elongated objects may be produced in a variety of different ways [13–17]. Both length dispersity and alignment affect the electrical conductivity of the samples [18,19].

Study of the percolation of rodlike particles or sticks in 2D systems and its connection with the electrical conductivity has a long history [20–22]. At present, the best known value of the percolation threshold in the 2D system of randomly oriented and placed zero-width sticks of equal length is 5.637 285 8(6) sticks per unit area [23]. The number of objects per unit area is also known as the number density.

A computer study of the percolation threshold in a two-dimensional anisotropic system of conducting sticks has been performed [24]. Here two kinds of angle distributions were taken into consideration, viz., uniform distribution within an interval

$$-\theta_m \leqslant \theta \leqslant \theta_m \tag{1}$$

and the normal distribution; log-normal distribution of lengths was assumed. An analytical relationship between the critical density of sticks and anisotropy has been proposed. This relation predicts that the percolation threshold will increase with increasing anisotropy from its isotropic value. Obviously, in a system of completely aligned, i.e., parallel, sticks, no percolation can occur.

The conductivity of stick percolation clusters with anisotropic alignments has been studied by means of computer simulation and finite-size scaling analysis [25]. The angular distribution of the sticks corresponds to (1). The critical number density n_c does not vary much for $\theta_m \in (5\pi/18, \pi/2]$, while it changes rapidly as

$$n_c \sim \theta_m^{-0.9} \tag{2}$$

for $\theta_m < 5\pi/18$. The percolation threshold (critical number density) increases rapidly as the anisotropy is increased.

The finite continuum percolation of rectangles with different aspect ratios has been studied using their angular distribution [26]

$$f_\theta(\theta) = \frac{\Gamma\left(\frac{\alpha}{2}+1\right)}{\sqrt{\pi}\,\Gamma\left(\frac{\alpha+1}{2}\right)} \cos^\alpha\theta, \quad \theta \in \left[-\frac{\pi}{2}, \frac{\pi}{2}\right).$$

The parameter α controls the degree of anisotropy of the system. Here $\alpha = 0$ corresponds to a uniform distribution $f_\theta(\theta) = \pi^{-1}$ and hence to an isotropic system. The larger the value of α, the stronger the anisotropy. In addition, $\alpha = \infty$ corresponds to a full alignment of the sticks along the x axis.

Furthermore, the effect of the length dispersity of sticks on the percolation threshold has also been studied in several works. For instance, sticks with log-normal distributions of lengths were considered in [24]. The effects of length distribution, angular anisotropy, and wire curvature have been investigated both numerically and experimentally [27]. Each of these quantities was assumed to be normally distributed. The percolation threshold decreases as either the length or the angle dispersity increases. Furthermore, the cooperative influence of both effects, simultaneously, on the percolation threshold may be of special interest.

Percolation in systems of aligned rods with different aspect ratios has been simulated [28]. Both systems of rods of equal

*Corresponding author: tarasevich@asu.edu.ru
†dantealigjery49@gmail.com

length and systems consisting of mixtures of short and long rods were considered. Alignment of the rods led to increases in the percolation threshold. For mixtures of long and short rods, a nonmonotonic dependence of the percolation threshold on the fraction of short rods was demonstrated.

Numerical simulations of stick percolation have been performed [29] with uniform angular distributions of the sticks within a given interval as well as with normal distributions, while the stick lengths corresponded to a log-normal distribution. The probabilities of percolation were presented for different values of the parameters.

The goal of the present work is to obtain more accurate values for the dependences of the percolation thresholds on anisotropy and length dispersity. The rest of the paper is constructed as follows. In Sec. II, the technical details of the simulations and calculations are described. Section III presents our main findings. Section IV summarizes the main results.

II. METHODS

A. Preparation of the film samples

Zero-width (widthless) sticks were deposited randomly and uniformly with given anisotropy onto a substrate of size $L \times L$ having periodic boundary conditions, i.e., onto a torus. Intersections of the particles were allowed. The length of the particles l varied according to a log-normal distribution with the probability density function

$$f_l(l) = \frac{1}{l\sigma_l\sqrt{2\pi}} \exp\left(-\frac{(\ln l - \mu_l)^2}{2\sigma_l^2}\right). \tag{3}$$

The mean $\langle l \rangle$ and the standard deviation (SD) $\sigma(l)$ are connected with the parameters of the log-normal distribution μ_l and σ_l as

$$\langle l \rangle = \exp\left(\mu_l + \frac{\sigma_l^2}{2}\right), \tag{4}$$

$$\sigma(l)^2 = \left[\exp\left(\sigma_l^2\right) - 1\right] \exp\left(2\mu_l + \sigma_l^2\right). \tag{5}$$

A change of any parameter affects both the mean and the standard deviation. To avoid a superposition of different effects, the mean was set as a constant during the simulations. In this case, we could extract and study the individual effect of the length dispersity. All our computations were performed for $\langle l \rangle = 1$. For this particular value of the mean, the parameters of the log-normal distribution are

$$\mu_l = -\frac{\sigma_l^2}{2}, \quad \sigma_l^2 = \ln[\sigma(l)^2 + 1].$$

The anisotropy of the system is characterized by the order parameter (see, e.g., [30])

$$s = N^{-1} \sum_{i=1}^{N} \cos 2\theta_i, \tag{6}$$

where θ_i is the angle between the axis of the ith stick and the horizontal axis x and N is the total number of sticks in the system. Since for a uniform angular distribution within a symmetric interval (1)

$$s = \frac{\sin 2\theta_m}{2\theta_m},$$

relation (2) can be rewritten as

$$n_c \sim (1 - s)^{-0.45}. \tag{7}$$

Furthermore, the macroscopic anisotropy

$$A = \frac{\langle l|\cos\theta|\rangle}{\langle l|\sin\theta|\rangle} \tag{8}$$

was used [24,29] to characterize the anisotropy of systems with length dispersity. Here $\langle\cdot\rangle$ denotes the mean value.

In our simulations, the angles were distributed according to a normal distribution [31]

$$f_\theta(\theta) = \frac{1}{\sqrt{-\pi \ln s}} \exp\left(\frac{\theta^2}{\ln s}\right). \tag{9}$$

For each sample, a sequence of random positions (two coordinates for each stick), orientations, and lengths was generated. This sequence was used to produce a film with the desired number density of sticks n,

$$n = \frac{N}{L^2}. \tag{10}$$

Since support of the log-normal distribution is $l \in (0, \infty)$, the probability that $l > L$ is finite, although very small. All sticks with $l > L$ were rejected for deposition and excluded from the sequence. We performed our simulations for different values of the order parameter and length dispersity, viz., $s = 0, 0.1, \ldots, 0.9$, and SD $\sigma = 0, 0.5, 1.0$.

B. Estimation of the percolation threshold

To check for any occurrences of wrapping clusters, we used the union-find algorithm [32,33] adopted for continuous percolation [23,34] and paired with the Machta algorithm [35]. Sticks were added one by one onto the substrate until a cluster wrapping around the torus in two directions had arisen. The algorithm treats a cluster as a wrapping cluster if it intersects itself after wrapping around the torus one or more times. Figure 1 demonstrates an example of a system under consideration with intermediate values of the parameters ($s = 0.5$ and $\sigma = 0.5$) exactly at the percolation threshold (the number of sticks is 4833 and $n_c \approx 4.72$). The dashed lines correspond to the borders of the system under consideration. Periodic boundary conditions are applied to these borders, i.e., if a stick intersects a border, and its outer part is transferred to the opposite border; in other words, the stick transforms into two shorter sticks with touching opposite borders of the system from its inside. The resulting critical number density is averaged over 10^5 independent runs to obtain the probability of percolation $R_{N,L}$.

To obtain the probability $R(n, L)$ of percolation in the grand canonical ensemble, we convolved $R_{N,L}$ with the Poisson distribution [23,34]

$$R(n, L) = \sum_{N=0}^{\infty} \frac{\lambda^N e^{-\lambda}}{N!} R_{N,L}. \tag{11}$$

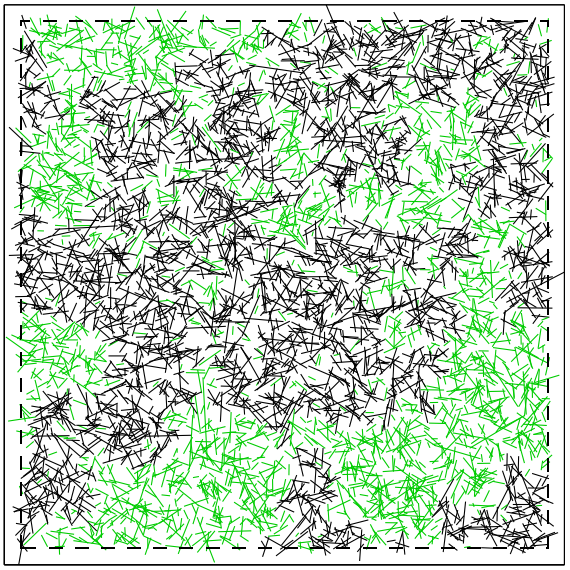

FIG. 1. Example of a system under consideration with intermediate values of the parameters $s = 0.5$ and $\sigma = 0.5$ for $L = 32$. The number density corresponds to the percolation threshold. The incipient wrapping cluster is shown in black.

Note that

$$\sum_{N=0}^{\infty} \frac{\lambda^N e^{-\lambda}}{N!} = 1 \,\forall \lambda > 0.$$

The weights in Eq. (11), $w_N(\lambda) = \lambda^N/N!$, can be calculated using the recurrent relations [23]

$$w_{\bar{N}-k} = \begin{cases} 1 & \text{for} \quad k = 0, \\ \frac{\bar{N}-k+1}{\lambda} w_{\bar{N}-k+1} & \text{for} \quad k = 1, 2, \ldots \end{cases} \tag{12}$$

and

$$w_{\bar{N}+k} = \begin{cases} 1 & \text{for} \quad k = 0, \\ \frac{\lambda}{\bar{N}+k} w_{\bar{N}+k-1} & \text{for} \quad k = 1, 2, \ldots . \end{cases} \tag{13}$$

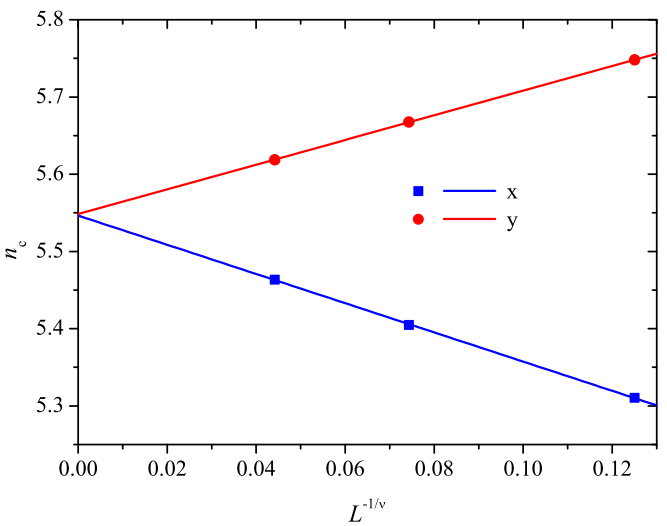

FIG. 2. Example of scaling for $s = 0.5$ and $\sigma = 0.5$.

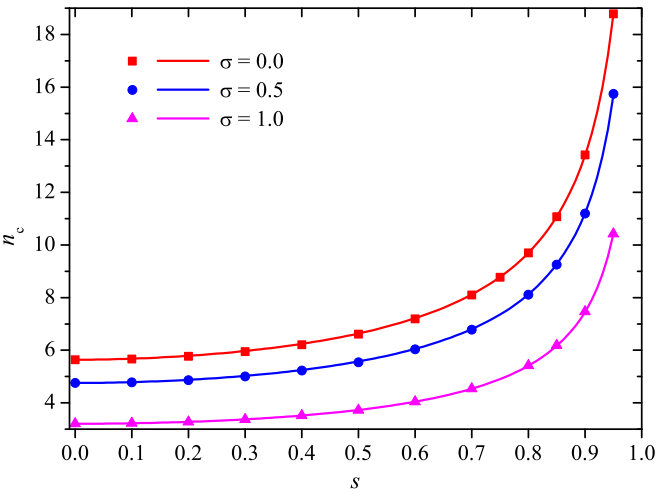

FIG. 3. Dependences of the percolation threshold n_c on the order parameter s for different values of SD σ. The curve corresponds to the least-squares fit (17).

Here the relation $\sum_{N=0}^{\infty} w_N(\lambda) = e^{\lambda}$ should be borne in mind. In addition, $\bar{N} = \lfloor \lambda \rfloor$. Therefore, the convolution can be calculated as

$$R(n, L) = \sum_{N=0}^{\infty} w_N^*(\lambda) R_{N,L}, \tag{14}$$

where

$$w_N^*(\lambda) = \frac{w_N(\lambda)}{\sum_{N=0}^{\infty} w_N(\lambda)}. \tag{15}$$

Since

$$\sum_{N=0}^{\infty} w_N(\lambda) = e^{\lambda} \sum_{N=0}^{\infty} w_N^*(\lambda),$$

$e^{-\lambda}$ is absent in the master equation (14).

Unfortunately, conformal field theory gives exact values for the wrapping probabilities at the transition in the limit

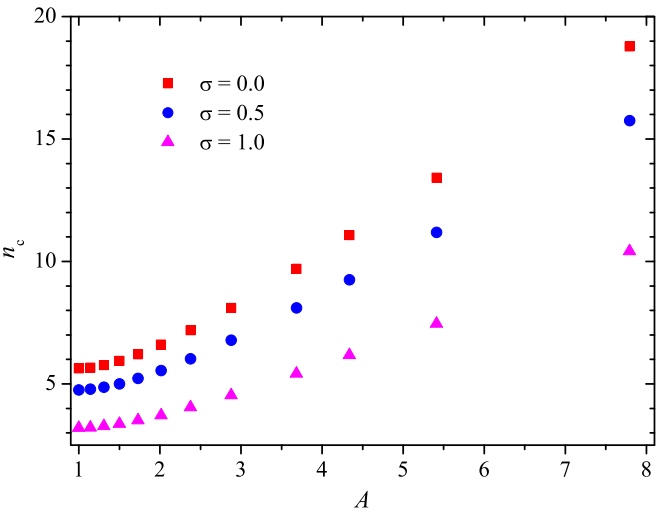

FIG. 4. Dependences of the percolation threshold n_c on the macroscopic anisotropy A for different values of SD σ.

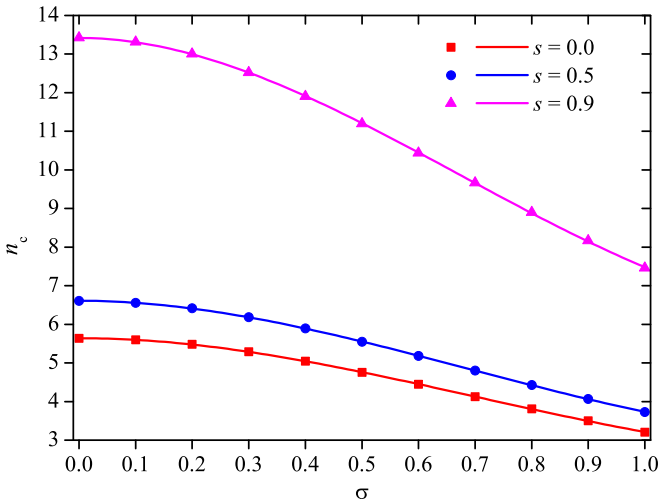

FIG. 5. Dependences of the percolation threshold n_c on the SD of the length dispersity σ for different values of the order parameter s. The curve corresponds to the least-squares fit (18).

$L \to \infty$ only for isotropic systems [32,33,36]. The most effective method to estimate the percolation threshold [23,32–34] does not work when the system is anisotropic. This is the reason why a different, less efficient, approach is used in our study. For each particular value of L, the equation $R(n_c, L) = 0.5$ is solved numerically using bisection. Then the scaling relation [1] is applied to find the percolation threshold in the thermodynamic limit

$$n_c(\infty) - n_c(L) \propto L^{-1/\nu}, \tag{16}$$

where $\nu = 4/3$. We use $L = 16, 32, 64$ to perform the scaling analysis; an additional size $L = 128$ is used for the set of parameters $s = 0$ and $\sigma = 0$. Figure 2 demonstrates an example of scaling for $s = 0.5$ and $\sigma = 0.5$. All results presented in Sec. III correspond to the thermodynamic limit. The error bars are of the order of the marker size.

III. RESULTS

Figure 3 demonstrates the dependence of the percolation threshold $n_c(s, \sigma)$ on the order parameter s for different values of SD σ. For any value of SD, the critical number density increases as the order parameter increases. The curves are fitted by

$$n_c(s, \sigma) = \frac{n_c(0, \sigma)}{\sqrt{1 - s^{\alpha}}}, \tag{17}$$

where the fitting coefficient α depends on SD σ (see Table I). From the nature of this case, $n_c(1, \sigma) = \infty$, since percolation of parallel zero-width sticks is impossible for any finite value of the number density. The asymptotic behavior $n_c(s \to 1, 0)$ corresponds to (7).

TABLE I. Fitting parameter α in (17) and $n_c(0, \sigma)$ for different values of SD σ.

σ	$n_c(0, \sigma)$	α	R^2
0.0	5.63724(18)	1.8449(26)	0.99998
0.5	4.756(3)	1.880(5)	0.99993
1.0	3.21(1)	1.9371(12)	1

TABLE II. Fitting parameters a and b in (18) and $n_c(s, 0)$ for different values of the order parameter s.

s	$n_c(s, 0)$	a	b	R^2
0.0	5.63724(18)	−4.59(3)	2.16(3)	0.99995
0.5	6.6076(4)	−5.57(4)	2.69(4)	0.99996
0.9	13.422(4)	−11.72(9)	5.78(9)	0.99994

Figure 4 shows the dependences of the percolation threshold n_c on the macroscopic anisotropy A for different values of SD σ. For the values of the macroscopic anisotropy $A \gtrapprox 3$, the dependences look almost linear. However, any conclusion regarding their asymptotic behavior ($A \to \infty$) is not really possible.

Figure 5 demonstrates the dependences of the percolation threshold $n_c(s, \sigma)$ on the SD σ for different values of the order parameter s. For any value of s, the critical number density decreases as the order parameter increases. This behavior is not unexpected, since long sticks may appear when the length dispersity is large. These long sticks may assist the development of a percolating cluster even at low number densities. The curves are fitted by

$$n_c(s, \sigma) = n_c(s, 0) + a\sigma^2 + b\sigma^3, \tag{18}$$

where the fitting parameters a and b depend on s (see Table II).

IV. CONCLUSION

By means of computer simulation and scaling analysis, we studied the percolation of zero-width sticks on a plane, paying special attention to the cooperative effects of both the

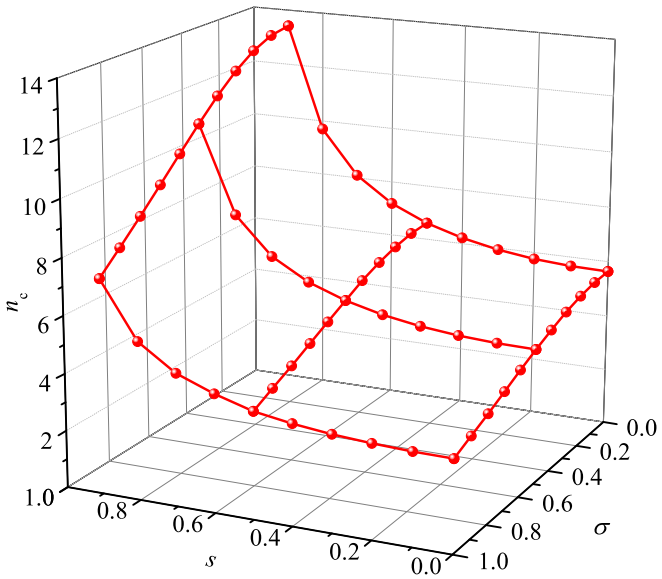

FIG. 6. Dependence of the percolation threshold n_c on both the order parameter s and the SD σ.

alignment of sticks and their length dispersity on the percolation threshold. The dependences of the percolation threshold on the alignment of the rods and their length dispersity have been obtained in the thermodynamic limit. Figure 6 demonstrates the dependence of the percolation threshold n_c on both the order parameter s and on the SD σ. The highest values of the percolation threshold correspond to highly anisotropic systems with equal-sized sticks, while the lowest values correspond to isotropic systems with high length dispersity. The percolation threshold can be fitted as

$$n_c(s,\sigma) = \frac{n_c(0,0) + a\sigma^2 + b\sigma^3}{\sqrt{1-s^\alpha}},$$

where the coefficients a and b should be taken from the first row of Table II and $\alpha = 1.8449 + 0.0493\sigma + 0.04289\sigma^2$. An obvious drawback of our study is its consideration of only one particular kind of angular distribution and only one particular kind of length distribution. Nevertheless, we consider the chosen distributions as the most natural. For other kinds of physically reasonable distributions, similar behavior of the percolation threshold is expected.

ACKNOWLEDGMENT

We acknowledge funding from the Ministry of Education and Science of the Russian Federation, Project No. 3.959.2017/4.6.

[1] D. Stauffer and A. Aharony, *Introduction to Percolation Theory* (Taylor & Francis, London, 1992).
[2] M. Sahimi, *Applications of Percolation Theory* (Taylor & Francis, London, 1994).
[3] B. Bollobás and O. Riordan, *Percolation* (Cambridge University Press, Cambridge, 2006).
[4] G. R. Grimmett, *Percolation* (Springer, Berlin, 1999).
[5] H. Kesten, in *Percolation Theory for Mathematicians*, edited by P. Huber and M. Rosenblatt Progress in Probability and Statistics (Birkhäuser, Boston, 1982), Vol. 2.
[6] R. M. Mutiso and K. I. Winey, Electrical properties of polymer nanocomposites containing rod-like nanofillers, Prog. Polym. Sci. **40**, 63 (2015).
[7] A. Kumar and G. U. Kulkarni, Evaluating conducting network based transparent electrodes from geometrical considerations, J. Appl. Phys. **119**, 015102 (2016).
[8] A. Kumar, N. S. Vidhyadhiraja, and G. U. Kulkarni, Current distribution in conducting nanowire networks, J. Appl. Phys. **122**, 045101 (2017).
[9] A. V. Kyrylyuk and P. van der Schoot, Continuum percolation of carbon nanotubes in polymeric and colloidal media, Proc. Natl. Acad. Sci. USA **105**, 8221 (2008).
[10] K. Gnanasekaran, G. de With, and H. Friedrich, On packing, connectivity, and conductivity in mesoscale networks of polydisperse multiwalled carbon nanotubes, J. Phys. Chem. C **118**, 29796 (2014).
[11] J. W. Borchert, I. E. Stewart, S. Ye, A. R. Rathmell, B. J. Wiley, and K. I. Winey, Effects of length dispersity and film fabrication on the sheet resistance of copper nanowire transparent conductors, Nanoscale **7**, 14496 (2015).
[12] M. Majidian, C. Grimaldi, L. Forró, and A. Magrez, Role of the particle size polydispersity in the electrical conductivity of carbon nanotube-epoxy composites, Sci. Rep. **7**, 12553 (2017).
[13] Z. Chen, W. Hu, J. Guo, and K. Saito, Fabrication of nanoelectrodes based on controlled placement of carbon nanotubes using alternating-current electric field, J. Vac. Sci. Technol. B **22**, 776 (2004).
[14] F. Du, J. E. Fischer, and K. I. Winey, Effect of nanotube alignment on percolation conductivity in carbon nanotube/polymer composites, Phys. Rev. B **72**, 121404 (2005).
[15] C. Park, J. Wilkinson, S. Banda, Z. Ounaies, K. E. Wise, G. Sauti, P. T. Lillehei, and J. S. Harrison, Aligned single-wall carbon nanotube polymer composites using an electric field, J. Polym. Sci. B **44**, 1751 (2006).
[16] A. Behnam, J. Guo, and A. Ural, Effects of nanotube alignment and measurement direction on percolation resistivity in single-walled carbon nanotube films, J. Appl. Phys. **102**, 044313 (2007).
[17] D. Yang, L. Wang, X. Zhang, D. Wang, Z. Shen, and S. Li, Alignment of nanoscale single-walled carbon nanotubes strands, Nano-Micro Lett. **3**, 146 (2011).
[18] J. Hicks, A. Behnam, and A. Ural, Resistivity in percolation networks of one-dimensional elements with a length distribution, Phys. Rev. E **79**, 012102 (2009).
[19] T. Ackermann, R. Neuhaus, and S. Roth, The effect of rod orientation on electrical anisotropy in silver nanowire networks for ultra-transparent electrodes, Sci. Rep. **6**, 34289 (2016).
[20] G. E. Pike and C. H. Seager, Percolation and conductivity: A computer study. I, Phys. Rev. B **10**, 1421 (1974).
[21] I. Balberg and S. Bozowski, Percolation in a composite of random stick-like conducting particles, Solid State Commun. **44**, 551 (1982).
[22] I. Balberg, N. Binenbaum, and C. H. Anderson, Critical Behavior of the Two-Dimensional Sticks System, Phys. Rev. Lett. **51**, 1605 (1983).
[23] S. Mertens and C. Moore, Continuum percolation thresholds in two dimensions, Phys. Rev. E **86**, 061109 (2012).
[24] I. Balberg and N. Binenbaum, Computer study of the percolation threshold in a two-dimensional anisotropic system of conducting sticks, Phys. Rev. B **28**, 3799 (1983).
[25] S.-H. Yook, W. Choi, and Y. Kim, Conductivity of stick percolation clusters with anisotropic alignments, J. Korean Phys. Soc. **61**, 1257 (2012).
[26] M. A. Klatt, G. E. Schröder-Turk, and K. Mecke, Anisotropy in finite continuum percolation: Threshold estimation by Minkowski functionals, J. Stat. Mech. (2017) 023302.
[27] D. P. Langley, M. Lagrange, N. D. Nguyen, and D. Bellet, Percolation in networks of 1-dimensional objects: Comparison between Monte Carlo simulations and experimental observations, Nanoscale Horiz. **3**, 545 (2018).
[28] A. P. Chatterjee, Percolation in polydisperse systems of aligned rods: A lattice-based analysis, J. Chem. Phys. **140**, 204911 (2014).
[29] J. L. Mietta, R. M. Negri, and P. I. Tamborenea, Numerical simulations of stick percolation: Application to the study of structured magnetorheological elastomers, J. Phys. Chem. C **118**, 20594 (2014).

[30] D. Frenkel and R. Eppenga, Evidence for algebraic orientational order in a two-dimensional hard-core nematic, Phys. Rev. A **31**, 1776 (1985).

[31] N. I. Lebovka, Y. Y. Tarasevich, N. V. Vygornitskii, A. V. Eserkepov, and R. K. Akhunzhanov, Anisotropy in electrical conductivity of films of aligned intersecting conducting rods, Phys. Rev. E **98**, 012104 (2018).

[32] M. E. J. Newman and R. M. Ziff, Efficient Monte Carlo Algorithm and High-Precision Results for Percolation, Phys. Rev. Lett. **85**, 4104 (2000).

[33] M. E. J. Newman and R. M. Ziff, Fast Monte Carlo algorithm for site or bond percolation, Phys. Rev. E **64**, 016706 (2001).

[34] J. Li and S.-L. Zhang, Finite-size scaling in stick percolation, Phys. Rev. E **80**, 040104 (2009).

[35] J. Machta, Y. S. Choi, A. Lucke, T. Schweizer, and L. M. Chayes, Invaded cluster algorithm for Potts models, Phys. Rev. E **54**, 1332 (1996).

[36] H. T. Pinson, Critical percolation on the torus, J. Stat. Phys. **75**, 1167 (1994).